MQP-ID-DSA-9464

# MUTAGENESIS OF HUMAN SUPERVILLIN'S ADHESION SEQUENCE IDENTIFIES CHANGES IN THE NUMBER OF CELLS CONTAINING STRESS FIBERS

A Major Qualifying Project Report

Submitted to the Faculty of the

WORCESTER POLYTECHNIC INSTITUTE

in partial fulfillment of the requirements for the

Degrees of Bachelor of Science

in

Biochemistry

and

Biology and Biotechnology

by

Michelangela Yusif

April 25, 2013

APPROVED:

| | | |
|---|---|---|
| Elizabeth Luna, PhD<br>Cell Biology<br>UMass Medical School<br>MAJOR ADVISOR | David Adams, PhD<br>Biology and Biotech<br>WPI Project Advisor | Destin Heilman, PhD<br>Chemistry and Biochemistry<br>WPI Project Advisor |

# ABSTRACT

A focal adhesion targeting sequence within the protein supervillin regulates the turnover of focal adhesions and its associated actin-rich stress fibers. The 1000 Genomes Project identifies naturally occurring human variations within this sequence. Point mutagenesis was undertaken to determine if these human variations affect stress fiber formation in transfected COS7-2 mammalian cells. The data suggest that hSV down-regulates stress fiber counts along with the naturally occurring variant of G466R; whereas RY/AA produces results similar to those depicted in bSV, and T426A increases stress fiber counts.

# TABLE OF CONTENTS

# ACKNOWLEDGEMENTS

I would like to thank Dr. Elizabeth Luna of the University of Massachusetts Medical School for giving me the opportunity me to work in her laboratory and for all the guidance received throughout this project. I would like to also thank her for all the weekends she spent with me in lab, allowing me to fully use the laboratory, and reviewing my report. I thank Tara C. Smith, Research Associate, for all the countless hours and late nights she spent with me in the laboratory to help me understand each step of the protocols. In addition, I thank Zhiyou Fang, PostDoc, and Kay Son, visiting associate Professor, for helping me with impromptu questions about laboratory protocols. I would like to thank Jeanette Campbell for her help on the project. Last but not least, I would like to thank my WPI Advisors, Professors Dave Adams and Destin Heilman for generating questions and assisting me with possible solutions to problems encountered during the project; I would also like to thank them for editing my final MQP report.

# BACKGROUND

## Myofibrils

Within the human body, all cells are being replenished with oxygen from the heart. The latter organ contracts and relaxes to enable the flow of oxygenated blood to the rest of the body as deoxygenated blood flows back into it. Cardiomyocytes, mononucleated striated heart muscle cells, allow for the heart to perform such a function (Cox et al., 2008). These cells along with all muscle cells are composed of myofibrils containing sarcomeres, multi-protein complexes which allow for the contraction of the cell (Cooper, 2000).

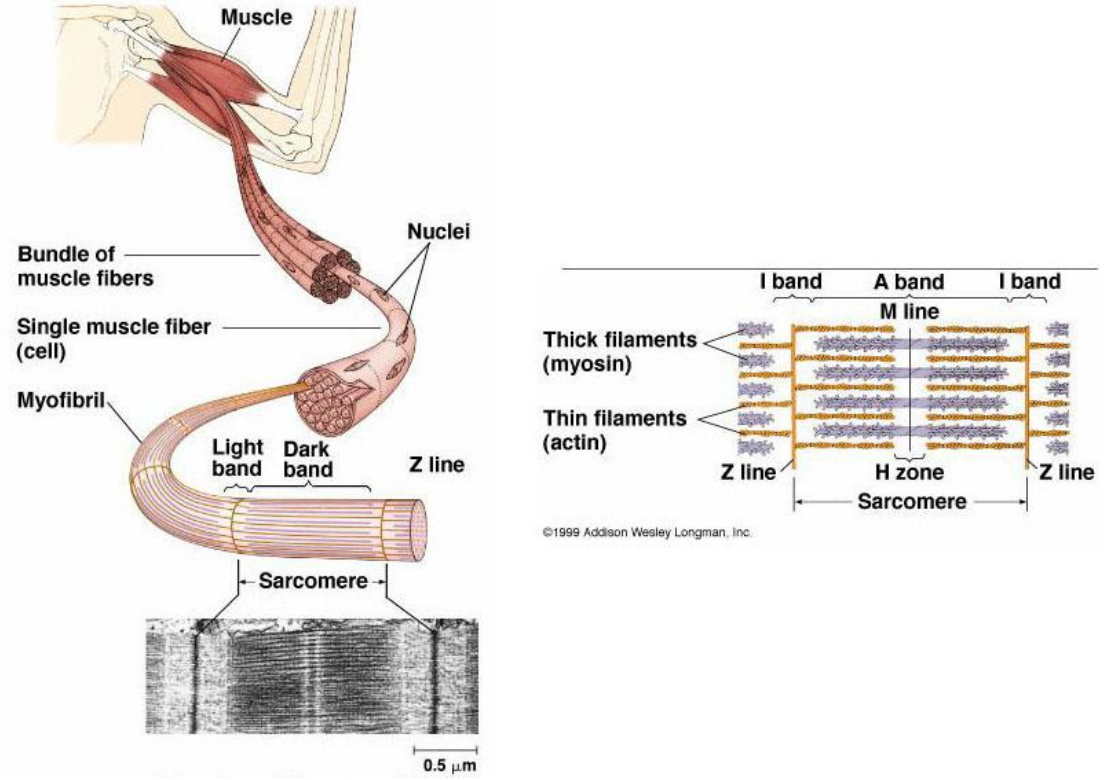


Figure1. Schematic of the human muscle from its bundle of fibers to its subnuclear components of actin and myosin filaments (King, 2013).

Thick myosin and thin actin filaments are the two main components in a sarcomere but the latter can be divided into four different sections (Cox et al., 2008). Mechanical joints of Z-discs or Z-lines separate sarcomeres from each other and are connected to actin-based thin filaments, whereas the M line or H zone (area surrounding M line) is constituted of bipolar myosin-based thick filaments and lies in the center of the sarcomere as shown in **Figure 1** (King, 2013). Isotropic bands (I bands) with thin filaments of opposite polarity surround Z-discs and lie on each side of anisotropic (A bands) bands composed of interdigitating thin and thick filaments (Cooper, 2000). As described in Huxley's sliding-filament model (Huxley et al., 1954), muscle contraction is caused by the sliding of the myosin filaments in both directions along the thin filaments, as depicted in **Figure 2** (Cooper, 2000).

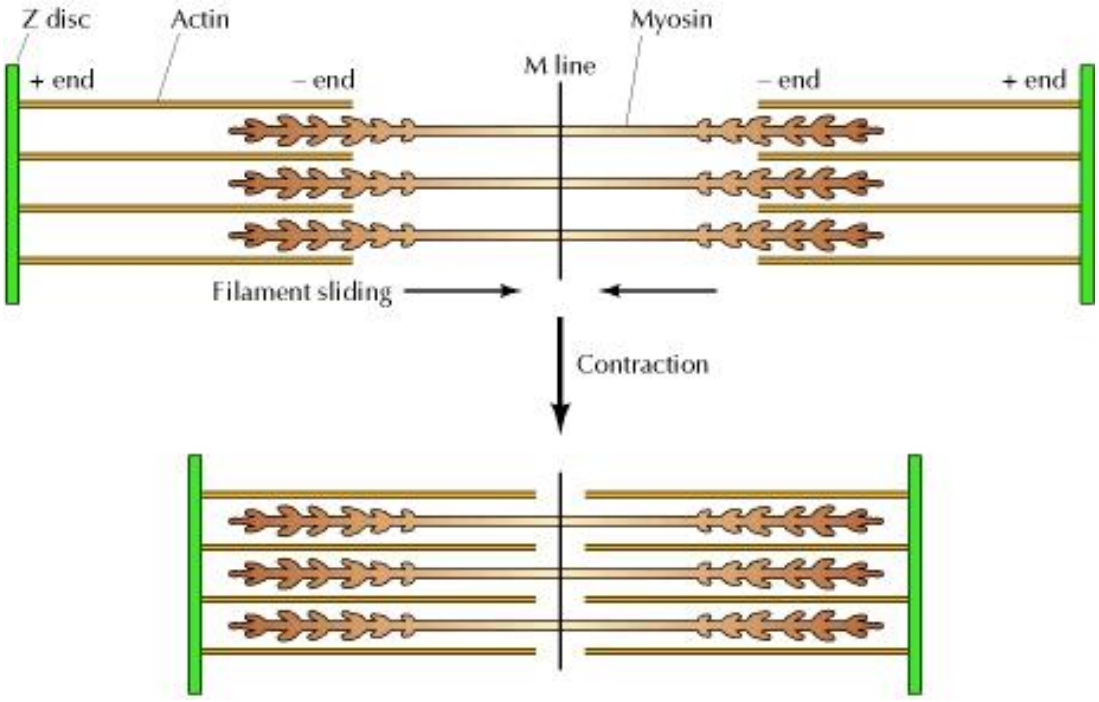


Figure 2. Schematic of sliding-filament model of myosin and actin filaments (Cooper, 2000).

As the contractile forces shorten the sarcomere, the muscle cell's plasma membrane (sarcolemma) remains attached to the myofibrils at specialized structures, called costameres, which link the extracellular matrix (ECM) to the Z-discs and M-lines (Cutroneo et al., 2011).

## Costameres

Many congenital muscle diseases arise from defects in structural proteins at costameres. These sites are stabilized and regulated by two major protein complexes: dystrophin/ sarcoglycan and integrin-based structures reminiscent of focal adhesions in nonmuscle cells, as shown in **Figure 3** below (Samarel et al., 2005; Ervasti et al., 2003).

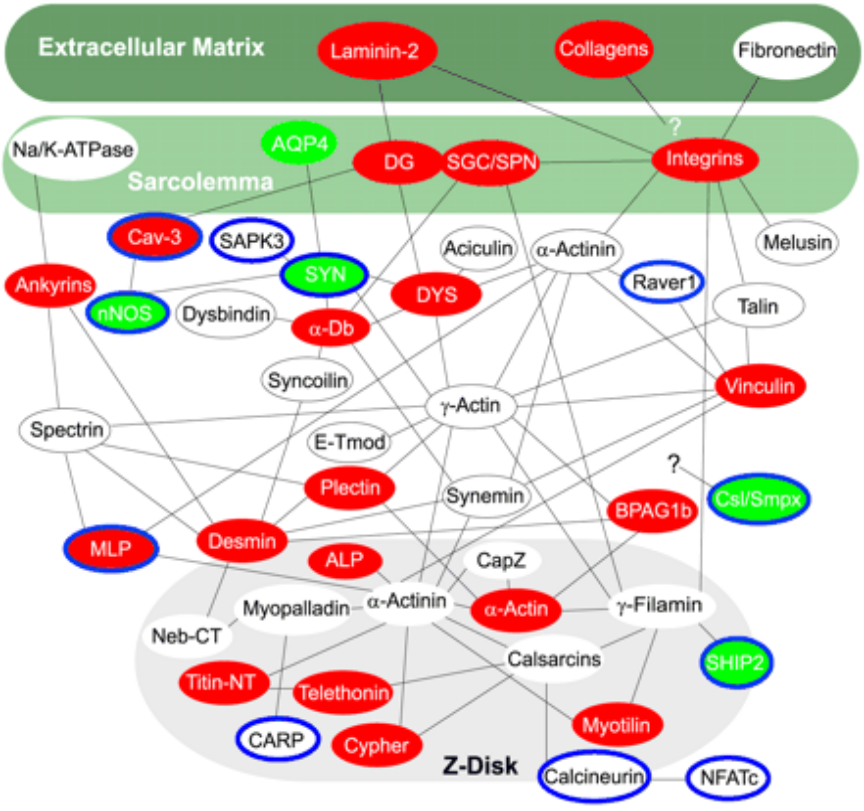


Figure 3. Proteins interaction allowing attachment of sarcolemma and Z-disks along with Interactions between the sarcolemma and the extracellular matrix (Evarsti, 2003).

Through screening the muscle biopsies of 204 patients for α-sarcoglycan deficiency, Fanin et al. discovered that mutations in the sarcoglycan complexes gene are the causes for autosomal recessive limb-girdle muscular dystrophies (Fanin et al., 1997). Upon observing the percentages of mutations in different sarcoglycan complexes among the patients screened, α-sarcoglycan was found to be the most commonly mutated protein complex (Fanin et al., 1997). Studies in mouse models have shown that mutations in Z-disc and/or costameric proteins lead to weakening of heart muscles (cardiomyopathy) and heart failure due to loss of structural integrity and signaling of the cardiomyocytes (Cox et al., 2008). Genetic removal of the $\beta_1$ integrin in muscle causes defects in adhesion and cytoskeletal disorganization (Cox et al., 2008). Though further research it has been observed that sites connecting costameric complexes to the extracellular matrix are necessary for not only the normal function of heart cells but also for all muscle cells (Cutroneo et al., 2011).

## Focal Adhesions

Like muscle cells, nonmuscle cells also need focal adhesions (FAs) and actomyosin contractility for movement. Nonmuscle cell focal adhesions, **Figure 4** (Lo, 2006) are specialized adhesion sites that provide communication between the cell and its ECM, regulate cytoskeletal structure, and mediate cell-ECM force transmission (Burridge et al., 1996; Kanchanawong et al., 2010). The cell's motility is accomplished through integrins, collection of receptors localized in the plasma membrane, which bind to ECM components on the outside (e.g. ligands) and trigger the formation of stress fibers, made of bundles of actin filaments, on the inside (Yamada and Miyamoto, 1995). Integrins are heterodimers of transmembrane α and β subunits. Most focal adhesion integrins contain

$\beta_1$ or $\beta_3$ subunits, which can bind a variety of ECM proteins through different αβ combinations. The α and β subunits usually contain large extracellular and short intracellular domains (Burridge et al., 1996). Integrin heterodimers continue to localize at FA after deletion of the $\beta_1$ cytoplasmic region and replacement with cytoplasmic domains from unrelated receptors (Geiger et al 1992; LaFlamme et al., 1992). The deletion of the cytoplasmic region of an α integrin tends to increase FA targeting (Briesewitz and Marcantonio, 1993; Ylainne et al., 1993). Thus, the cytoplasmic domain of β subunit promotes integrin targeting to FAs, whereas the α subunit of the cytoplasmic domain may even inhibit FA localization. Inhibition of the localization to FA by the α subunit of the cytoplasmic domain can be prevented through ligand binding (LaFlamme et al., 1992). Most FA cytoplasmic proteins interact directly or indirectly with actin filaments.

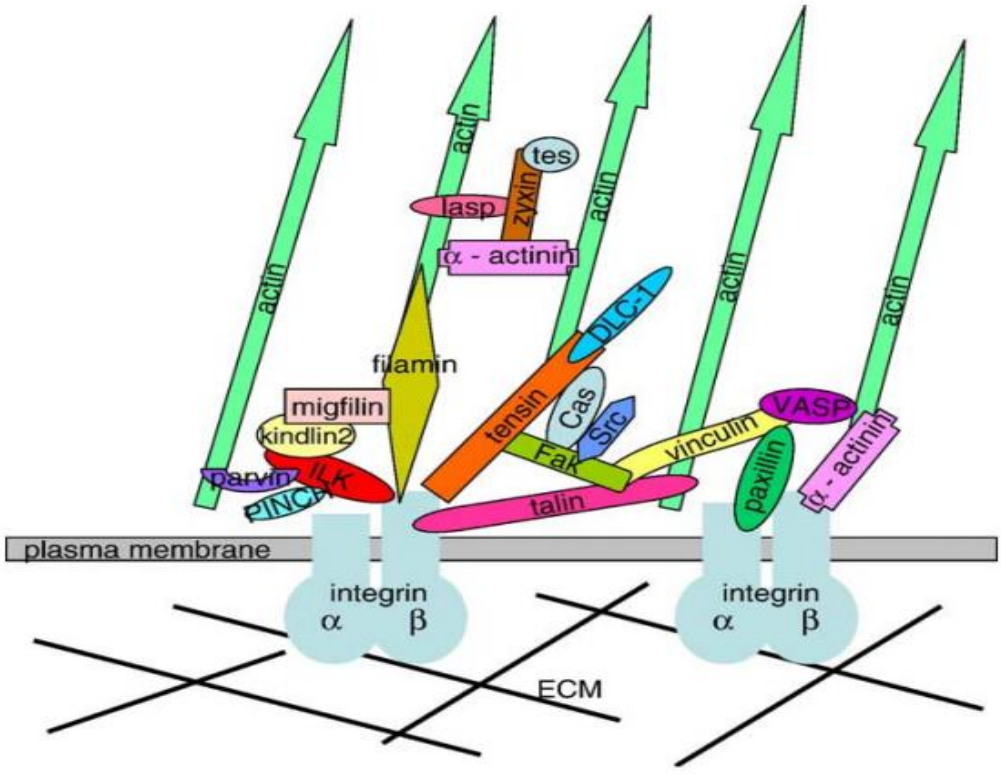


Figure 4. Focal adhesion site depicting interactions between intracellular components (top), transmembrane integrins and extracellular matrix (ECM, bottom) (Lo, 2006).

Focal adhesion proteins form very large structures (length of 40 nm) that link transmembrane integrins with actin filaments (Kanchanawong et al., 2010). Nascent focal adhesions form after binding of an extracellular ligand as shown in **Figure 4**. The integrin undergoes conformational changes as it becomes activated. The initially small focal complexes become enlarged as more binding partners are recruited and as integrins in the plane of the membrane become aggregated through numerous interactions with additional extracellular ligands and intracellular adapter proteins (Wehrle-Haller, 2012b; Galbraith et al., 2013). During migration, these structures change in composition, first recruiting and activating myosin II in order to pull the cell forward, and then maturing into signaling platforms before disassociating (Wehrle-Haller, 2012a). Myosin II activation promotes the recruitment of supervillin and calpain-2 into FA (Kuo et al., 2011). Calpain-2 is a protease that cleaves many FA cytoplasmic proteins (Kuo et al., 2011), starting a process that results in the disassembly and turnover of the components. As discussed below, supervillin also promotes FA disassembly, implicating myosin activation as a process that initiates both FA function and FA disassembly. The adapter proteins not only provide a positive feedback loop that increases cell spreading, but also recruit signaling proteins (Luxenburg et al., 2012). Aggregation increases the avidity of ECM-integrin binding at focal adhesions, but the highest affinity binding requires an additional energy-dependent step that is consistent with a requirement for activation of focal adhesion-associated myosin II (Schürpf and Springer, 2011).

Stress fibers are contractile actin and myosin II bundles in nonmuscle cells that are structured in a similar way as in muscle sarcomeres. Stress fibers contract in response to signals generated at focal adhesions (Burridge et al., 1996). Stress fiber formation in

cultured endothelial cells increases when the cells are under tension. When tension is applied to a specific area on the cell's surface, actin filament bundles form in that area. Disruption of focal adhesion and stress fiber formation has also been observed to be due to the binding competitiveness of a substrate to a domain. For example, Höner et al microinjected antibodies against the myosin rod domain which resulted in disruption of stress fibers due to no myosin filament assembly (Höner et al, 1988).

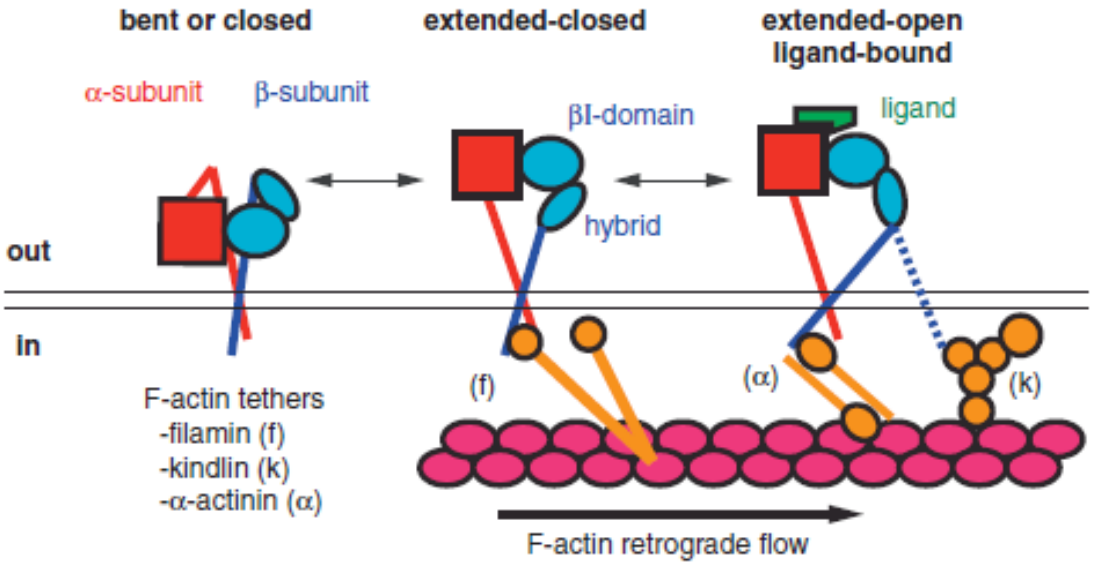


Figure 5. Conformational change of the α and β subunits of integrins. (Wehrle-Haller, 2012a)

Increased levels of cAMP (cyclic adenosine monophosphate) have also been observed to hinder aggregation of stress fibers. Throughout all the research conducted, it is reasonable to state that aggregation and formation of stress fibers and focal adhesion are primarily due to tension through contractility (Burridge et al., 1996).

## *Supervillin*

The regulation of a cell's movement is monitored by a wide variety of proteins. Supervillin (SV) is a peripheral membrane protein that down-regulates stress fibers, FAs, and adhesion between cells and substrates through interactions with myosin II and F-actin (Takizawa et al., 2006). Supervillin is a 205 kDa protein, with a long N-terminus that is mostly unstructured (Fedechkin et al., 2013) and a C-terminus with high homology to the villin family of actin-binding proteins (Pestonjamasp et al., 1997; Smith et al., 2010). Supervillin was first purified from bovine neutrophil plasma membranes (Pestonjamasp et al., 1997), but isoforms are present in most nonmuscle and muscle cells (Pope et al., 1998; Oh et al., 2003; Fang and Luna, 2013).

More than 95% of supervillin localizes and co-purifies with plasma membranes in differentiated cells (Nebl et al., 2002; Takizawa et al., 2007). Through tight binding with both F-actin and myosin II, SV regulates assembly of actin and myosin filaments at the membrane, generates bundles of actin filaments, cross-links F-actin, and activates myosin II (Chen et al., 2002/3; Bhuwania et al., 2012; Takizawa et al., 2006; Takizawa et al., 2007). Supervillin binding to focal adhesions is regulated by its interaction with thyroid receptor-interacting protein 6 (TRIP6) (Takizawa et al., 2006). Like supervillin, TRIP6 is located in mature focal adhesions and plays a role in both actin filament organization and cell migration (Takizawa et al., 2006). The TRIP6-binding sequence within SV lies within supervillin amino acid residues 342 through 571, near the protein's N-terminus.

Both SV and TRIP6 negatively affect large focal adhesions (Takizawa et al., 2006). Takizawa et al., 2006 and Wulfkuhle et al., 1999 have shown that SV localizes at or near mature FAs and decreases their number along with the numbers of FA-associated

stress fibers (Takizawa et al., 2006; Wulfkuhle et al., 1999). When SV is depleted by RNAi, cell-substrate adhesion increases. Through the reduction of stress fibers and FA, the cell loses tight binding to the substrate, potentially increasing the rate of cell motility. In fact, HeLa cells containing supervillin translocate faster than do supervillin-depleted cells (Fang et al., 2010). Overexpression of the evolutionarily conserved TRIP6-binding site, consisting of bovine supervillin (bSV) residues 343-571 (bSV343-571), disrupts FA formation even more effectively than does full-length supervillin (Chen et al., 2002/3; Takizawa et al., 2006). Mutations within this conserved region abolish the dominant-active decreases in stress fibers and large FA structures (Takizawa et al., 2006). Overexpression of TRIP6 constructs can rescue the effects of wild-type bSV343-571 constructs, suggesting that the effect on FA structure and function is mediated by the SV-TRIP6 interaction (Takizawa et al., 2006).

Supervillin sequences have been found in all vertebrates for which genomic sequences are available and in other species, including hagfish, sea urchins, worms, and flies. The C-terminal villin-like sequences in supervillin are even more highly conserved than is the unstructured N-terminus, with similarities to proteins found in worms, flies, and amoebae. However, the TRIP6-binding sequence is conserved only in vertebrate supervillins.

## *Human Supervillin*

Within the human body, there are four known isoforms of supervillin; these isoforms arise due to differential splicing of the single SVIL gene (Fang and Luna, 2013). The largest isoform, which is found in striated muscle, contains ~45 kDa of additional

amino acid sequence encoded by 4 exons. This isoform is known as archvillin (HAV, or supervillin isoform 2); supervillin isoform 1 (hSV1), with a mass of ~205 kDa, is the predominant isoform in most nonmuscle cells.

Until recently, nearly all studies have used bovine supervillin cDNAs. Although human supervillin was cloned and characterized by Pope et al. in 1998 (Pope et al., 1998), full-length hSV1 cDNA was not assembled until this year (Fang and Luna, 2013). The hSV1 N-terminus is 79.2% conserved with the N-terminus of bovine supervillin, and these two proteins are 95.1% identical in their C-termini. Full-length hSV1 protein is 1788 amino acids long and is found on the human chromosome at 10p11.2 (Pope et al., 1998). The TRIP6-binding site, which is 87.3% conserved between the species, is located at amino acids 342-571 and 339-569 for bSV and hSV, respectively (Pope et al., 1998). The 1000 Genomes Project website has documented approximately 293 naturally occurring variants in hSV which have been predicted to be possibly damaging. Several of these are located within or around the TRIP6-binding site, suggesting that these naturally occurring human variants may have differential effects of cell-substrate adhesion and stress fiber counts and, by extension, on supervillin function in muscle and nonmuscle tissues. Previous studies by Takizawa et al. using bSV have shown that the mutation of arginine 426 and tyrosine 427 into alanines (RY/AA) resulted in SF levels similar to that of wild type COS 7 cells (Takizawa et al., 2006).

# PROJECT PURPOSE

Most of the previously published work on supervillin used the bovine supervillin (bSV) sequences to explore the regulatory role of supervillin at focal adhesions, but a human supervillin (hSV) cDNA was recently cloned. The purpose of this project was to verify that the focal adhesion-targeting sequence of ~230 amino acids in hSV functions in the same way as the corresponding bSV sequence, and to determine whether naturally occurring variations in this hSV sequence affect its function at focal adhesions. PCR was used to generate both consensus and variant hSV sequences, and mammalian expression plasmids were constructed. A fluorescence-based assay with transfected COS7-2 African green monkey kidney cells was used to determine the effects of these constructs on stress fiber formation and, by inference, focal adhesion function.

# METHODS

*Identifying Mutations in Human Supervillin (hSV)*

The 1000 Genomes project was utilized to identify naturally occurring variants in the focal adhesion-targeting sequence of human supervillin (amino acids 339-569) that were predicted to affect protein function (browser.1000genomes.org/Homo_sapiens/ Search/Results? site=ensembl&q=svil). Nomenclature was assigned using the original one letter code of the amino acid, number of amino acid residue, and the one letter code of the mutated amino acid e.g. T355I designated the mutation of amino acid residue threonine 355 into isoleucine 355. An exception was made for the double mutation of R423A and Y424A which was named RYAA for brevity. The mutations chosen for initial investigation were T355I, S400P, R410W, RYAA, S446L, W505C, T426E, T426A, and G466R.

*Cloning of 0.7 kb Focal Adhesion-targeting Sequence*

The 0.7-kb focal adhesion-targeting sequence in human supervillin was generated in touchdown polymerase chain reaction (PCR) using *Pfu Turbo* Hotstart DNA Polymerase (Agilent Technologies), gene-specific primers and full-length human supervillin cDNA as template. Forward and reverse primers were manufactured by Integrated DNA Technologies and contained restriction enzyme sequences specific for *SalI* and *BamHI*, respectively. The PCR product was purified through a 0.5% agarose gel electrophoresis and 3'adenosine overhangs were added with *Taq* Polymerase (New England BioLabs). Ligation of the 700 bp insert into the pCR 2.1 TOPO vector was performed using Invitrogen's TA Cloning Kit (Invitrogen). Ligated vector was

transformed into chemically competent *Escherichia coli* TOPO10F' cells, and a blue-white screening was completed. The bacterial cells were grown, and DNA plasmids were purified from selected clones to obtain the plasmid DNA construct. To verify the size of the insert, the plasmid was digested by *EcoRI* and run on an agarose gel. The insert sequence was verified by forward and reverse DNA sequencing. Sequencing was performed by the Molecular Biology Core Laboratory at the University of Massachusetts Medical School from mixtures of purified plasmids and M13 Forward or M13 Reverse primers.

*Mutagenesis PCR and Cloning into pEGFP-C1*

Combinations of 18 forward and reverse primers containing the 9 desired mutations were designed by following the Primer Design Guidelines in the QuickChange Site-Directed Mutagenesis Kit (Stratagene). To prevent problems from primer characteristics such as mismatches in annealing temperatures, GC content, and formation of secondary structures (e.g. primer dimers and hairpin), each primer was analyzed using Primer Premier (Premier Software). The designed primers were then manufactured and purified by Integrated DNA Technologies and utilized for site-directed mutagenesis PCR using Stratagene's QuickChange Site-Directed Mutagenesis Kit. The DNA template used was pCR 2.1 TOPO ligated with the 700 bp hSV adhesion sequence. PCR reactions to generate RYAA, T426E, and T426A utilized 18 cycles, with an extension time of 5 minutes (approximately 1 minute/kb of plasmid) at 68˚C. PCR reactions for T355I, S400P, R410W, S446L, W505C, T426A (repeated trial), and G466R included 12 cycles and a 5-min extension. The parent plasmids were digested with *Dpn I* and the daughter (mutated) plasmids were transformed into XL1-Blue Supercompetent cells. Cells were

plated onto ampicillin-resistant Luria-Bertani (LB) agar plates. Plasmid purifications were performed using the QIAprep Spin Miniprep Kit High-Yield Protocol (Qiagen). A pEGFP-C1 plasmid and the parent and mutated plasmids were doubly digested with *SalI* and *BamHI*, and the products were run on a 0.5% agarose gel. Insert and vector bands were extracted from the gel and purified using the ZymoClean Gel DNA Recovery Kit (Zymo Research). The 700 bp hSV inserts from both the parental (wild-type) and mutated sequences were ligated into doubly digested pEGFP-C1 vector, transformed into XL1-Blue Supercompetent cells, and purified.

*Cell Culture, Transfection, and Staining*

COS 7-2 African Green Monkey kidney cells, which are SV40-transformed variants of CV-1 epithelial cells, were cultured in DMEM with 10% fetal bovine serum (FBS) and 1% PenStrep. Cells were passaged into six 60-mm dishes containing coverslips (22 $mm^2$, 1.5mm thick), grown at 37˚C with 5% $CO_2$ for 18 hours and transfected for 23 hours using Qiagen's Transient or Stable Transfection of Adherent Cells protocol, except that 1.5 µg of plasmid DNA was used instead of 1 µg. Cells were transfected with the following plasmids: pEGFP-C1 (negative control), EGFP-BSV (positive control of bovine supervillin), pEGFP-C1+hSV339-569, pEGFP-C1+hSV339-569-RYAA, pEGFP-C1+ hSV339-569-T426A, and pEGFP-C1+ hSV339-569-G466R. Dishes were removed from the 37°C incubator after transfection, and coverslips were transferred into wells in a 6-well plate. Coverslips were washed 2 times with pre-warmed (37˚C) phosphate-buffered saline (PBS; 2 ml/well/wash), fixed with 4% paraformaldehyde in PBS (1.5ml/well) for 10 minutes at room temperature, and rinsed 3 times with PBS (2ml/well/wash) for 5 minutes. Coverslips were then permeabilized with

0.1% Triton X-100 in PBS (1.5ml/well) for 3 minutes, rinsed 3 times with PBS (2ml/well/wash) for 5 minutes , and blocked with Blocking Buffer (1% BSA, 0.5% Tween-20, 0.02% sodium azide in PBS) at room temperature for 30 minutes. Cells were stained for F-actin with 100 µl of 1:200 Texas Red-labeled phalloidin in Blocking Buffer and incubated in the dark at room temperature for 45 minutes. After incubation, cells were rinsed 3 times with PBS (2ml/well/wash) for 5 minutes. Coverslips were then mounted onto microscope slides containing 7 µl of Slow Fade (Invitrogen) and sealed with nail polish at room temperature.

*Western Immunoblotting*

Proteins were extracted from cells grown and transfected in 60-mm dishes, using 5X Laemmli Sample Buffer (2% SDS, 10% Glycerol, 20 mM DTT, 0.002% bromophenol blue, 62.5 mM Tris-Cl, pH 6.8). Extracts were separated on a 12% polyacrylamide resolving gel, with a 5% polyacrylamide stacking gel, pH 8.8, and electrophoresed using a Tris-glycine running buffer, pH 8.3, for 90 minutes at 82 V. The gel was blotted onto a nitrocellulose membrane in Towbin Transfer Buffer (Towbin et al., 1979) for 18 hours at 75 V at 4 ˚C. The membrane was stained with 10 ml ATX Ponceau S red staining solution (Sigma-Aldrich) with gentle rocking for 10 minutes, rinsed 3 times with 18 megaOhm water, and scanned using a Xerox WorkCentre 4150. EGFP-tagged proteins were visualized with a 1:1000 dilution of a rabbit anti-GFP (D5.1) XP Rabbit mAb (Cell Signaling) in 5% low-fat milk in 1X TBST for 90 minutes and a 1:10000 dilution of a horseradish peroxidase (HRP)-labeled goat secondary antibody (Dα Rb-HRp from Jackson ImmunoResearch) for 45 minutes. The membrane was washed 3 times for 10 minutes with 1X TBST before and after incubation with secondary antibody.

Thermo Scientific's SuperSignal® West Femto Chemiluminescent Substrate protocol was followed to develop protein band/s. As a protein loading control, actin was detected on the same blot using a 1:3000 dilution of a mouse primary antibody against actin, clone C4 (Millipore) and a 1:10000 dilution of HRP-labeled goat secondary antibody (Dα M-HRp from Jackson ImmunoResearch). Bands were developed using SuperSignal® West Pico Chemiluminescent Substrate.

*Immunofluorescence microscopy*

Transfected cells with and without stress fibers were counted using a 100X Pan-NeoFluar oil immersion objective, N.A.1.3, on a Zeiss Axioskop fluorescence microscope with a RETIGA 1300 CCD camera. Images were captured using OpenLab Software. Transfected cells containing the plasmid fluoresced green when observed through the fluorescein filter set whereas the presence of stress fibers was visible as red fluorescence using a rhodamine filter set.

After the cells for each construct were counted (minimum of 100 transfected cells), numbers were normalized by diving the number of transfected cells either containing or lacking stress fibers by the total number of cells counted and multiplying the quotient by 100%. A repeated measures ANOVA was performed in the InStat 3.0 program (GraphPad Software) to compare the experimental values with the EGFP control.

# RESULTS

The main goal of this MQP project was to examine whether naturally occurring variants in the target focal adhesion sequence (TRIP6 binding site) in human supervillin would affect the percentages of transfected COS7-2 cells that contain stress fibers. This assay is simple to score and has been shown to predict TRIP6 binding and whether bovine supervillin can target to focal adhesions (Takizawa et al., 2006). As a positive control, the RY/AA mutation was made in human supervillin because this mutation in bovine supervillin is known to abolish focal adhesion targeting (Takizawa et al., 2006). The T426A mutation was made because phosphorylation of this residue, located within two residues of the RY site, is the residue in supervillin that is the most likely to be phosphorylated (www.phosphosite.org).

Out of the 293 mutations within human supervillin scored as potentially damaging (browser.1000genomes.org/Homo_sapiens/Search/Results?site=ensembl&q=svil), we selected for targeting 8 mutations within the predicted focal adhesion targeting site. Primers were designed for each of these mutations, and site-directed mutagenic PCR reactions were carried out. The G466R mutation was successfully incorporated in the time allotted for this phase of the project, as were the RY/AA and T426A mutations. A T426E mutation also was attempted, but was unsuccessful. The successfully mutagenized sequences were moved to the pEGFP-C1 mammalian expression vector and transfected into COS7-2 cells. Successful expression of appropriately sized EGFP-tagged proteins was verified by immunoblot analyses of cell lysates stained with anti-EGFP. Transfected COS7-2 cells also were stained with fluorescent phalloidin and scored for the presence of stress fibers.

*Identifying Mutations in Human Supervillin (hSV) and Site-directed Mutagenics PCR*

The 1000 genomes website was used to identify naturally occurring variants within the target focal adhesion of human supervillin (amino acid residues 339-569) which could be possibly damaging. All chosen amino acid residues changes were located around the RY/AA mutation, due to the known effects of this mutation in bSV (Takizawa et al., 2006). **Table 1** below shows the mutations chosen along with the amino acid residue change and the specific single nucleotide polymorphism (SNP).

**Table 1: Chart of the Naturally Occurring Supervillin Variants and other hSV Mutations Attempted.**

| NAME | MUTATION | SNP |
|---|---|---|
| T355I | Threonine → Isoleucine | ACA → ATA |
| S400P | Serine → Proline | TCC → CCC |
| R410W | Arginine →Tryptophan | CGG→ TGG |
| R423A<br>Y424A } RY/AA | Arginine → Alanine<br>Tyrosine →Alanine | CGC → GCC<br>TAT → GCT |
| T426A | Threonine → Alanine | ACT → GCT |
| T426E | Threonine → Glutamic Acid | ACT → GAA |
| S446L | Serine → Leucine | TCA → TTA |
| G466R | Glycine → Arginine | GGA → AGA |
| W505C | Tryptophan → Cysteine | TGG → TGT |

Upon choosing the mutations to be made, primers were designed with base pair changes surrounded by nucleotides that perfectly matched sequences in the 700 bp hSV cDNA template. Site-directed mutagenesis PCR using primers containing the mutation/s of interest was completed using the insert/vector construct as the template (refer to Materials and Methods). Non-mutated template was digested with *Dpn I* restriction enzyme, and the mutated PCR products were cloned into the TOPO vector. TOPOF' chemically competent cells were then transformed with the ligated TOPO vectors.

Individual colonies were selected, and mutated inserts were verified by DNA sequencing in both directions. Correctly mutated inserts were cut out of the TOPO vectors and ligated into identically restricted pEGFP-C1 vectors. The top, middle, and bottom panels in **Figure 6** show the DNA sequence reads of the mutated RY/AA, T426A, and G466R fragments (rows 1, 4, and 7, respectively).

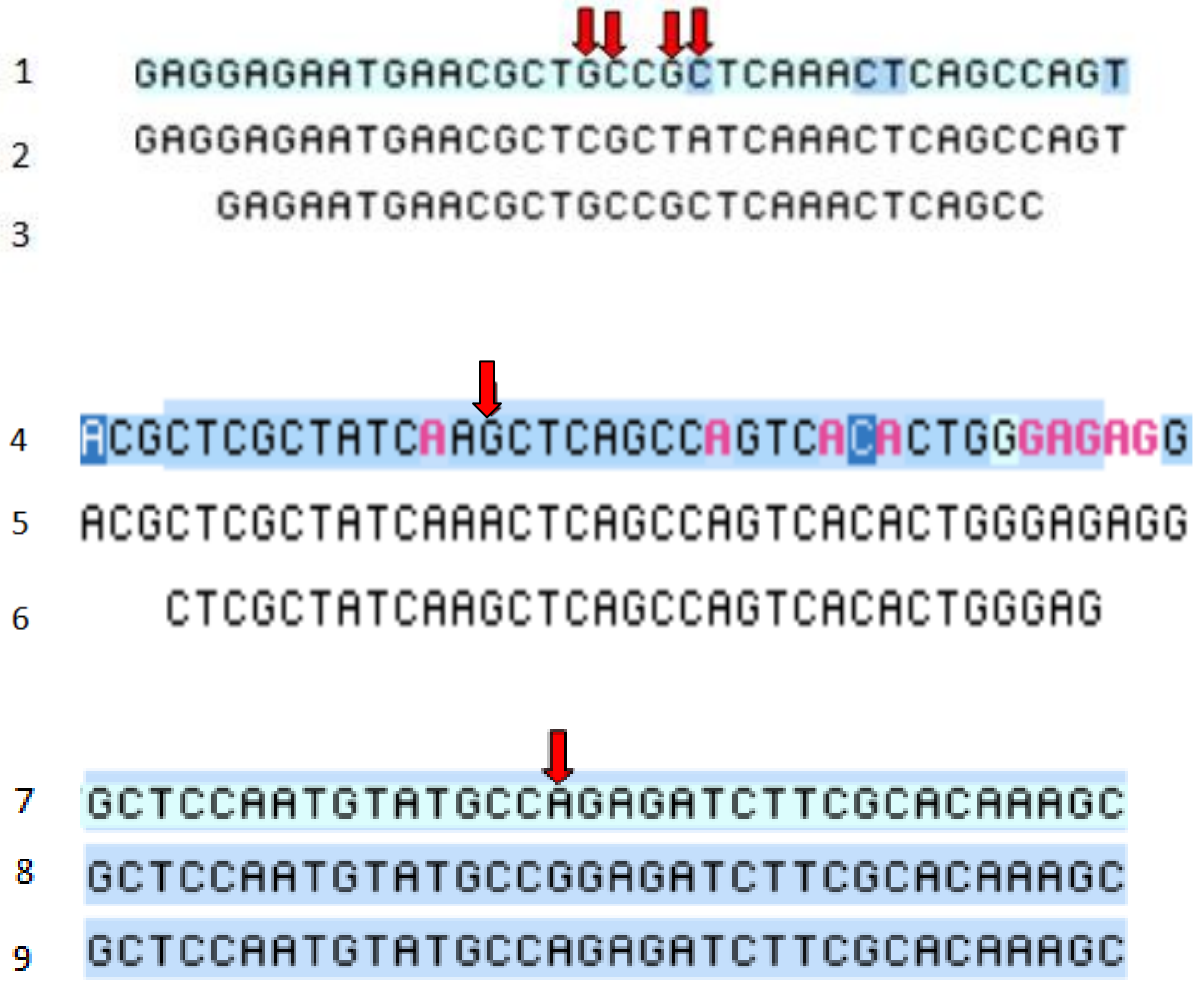


**Figure 6: Nucleotide Sequences.** Analysis and comparison of the sequence reads for hSV mutations, as compared with the parental hSV sequence and the mutagenic primers. Red arrows depict locations of the desired mutations.

The red arrows in the figure show the specific nucleotide changes for the mutations. Rows 2, 5, and 8 show the wild type/ unmutated hSV sequence, whereas rows 3, 6, and 9 depict the primers used for the site-directed mutagenesis PCR.

*Cell Culture, Transfection, and Staining*

After the COS 7-2 cells were grown in DMEM, FBS, and PenStrep (Materials and Methods), they were utilized for transfection using the following plasmid constructs: pEGFP-C1 (negative control), EGFP-BSV (positive control of bovine supervillin), pEGFP-C1+hSV339-569, pEGFP-C1+hSV339-569-RYAA, pEGFP-C1+hSV339-569-T426A, and pEGFP-C1+hSV339-569-G466R. For 23 hours, cells were allowed to divide, incorporate plasmid into their nuclei, and express protein. The cells then were fixed on the coverslip, permeabilized, stained, mounted onto microscope slides, and the numbers of transfected cells that contained and did not contain stress fibers were counted. **Figure 7**, below, shows representative pictures of each population of transfected cells, taken with a 100X objective lens. The first column shows the green fluorescence of transfected cells (EGFP Green column; viewed through the fluorescein filter), whereas the middle column in magenta shows the presence or absence of stress fibers (F-actin; imaged through a rhodamine filter set). The last column shows composites of the two superimposed channels; overlaps appear in white. Each row correlates with the EGFP-tagged hSV construct indicated. The histogram in **Figure 7** shows the average percentage of triplicate samples for the transfected cells containing stress fibers.

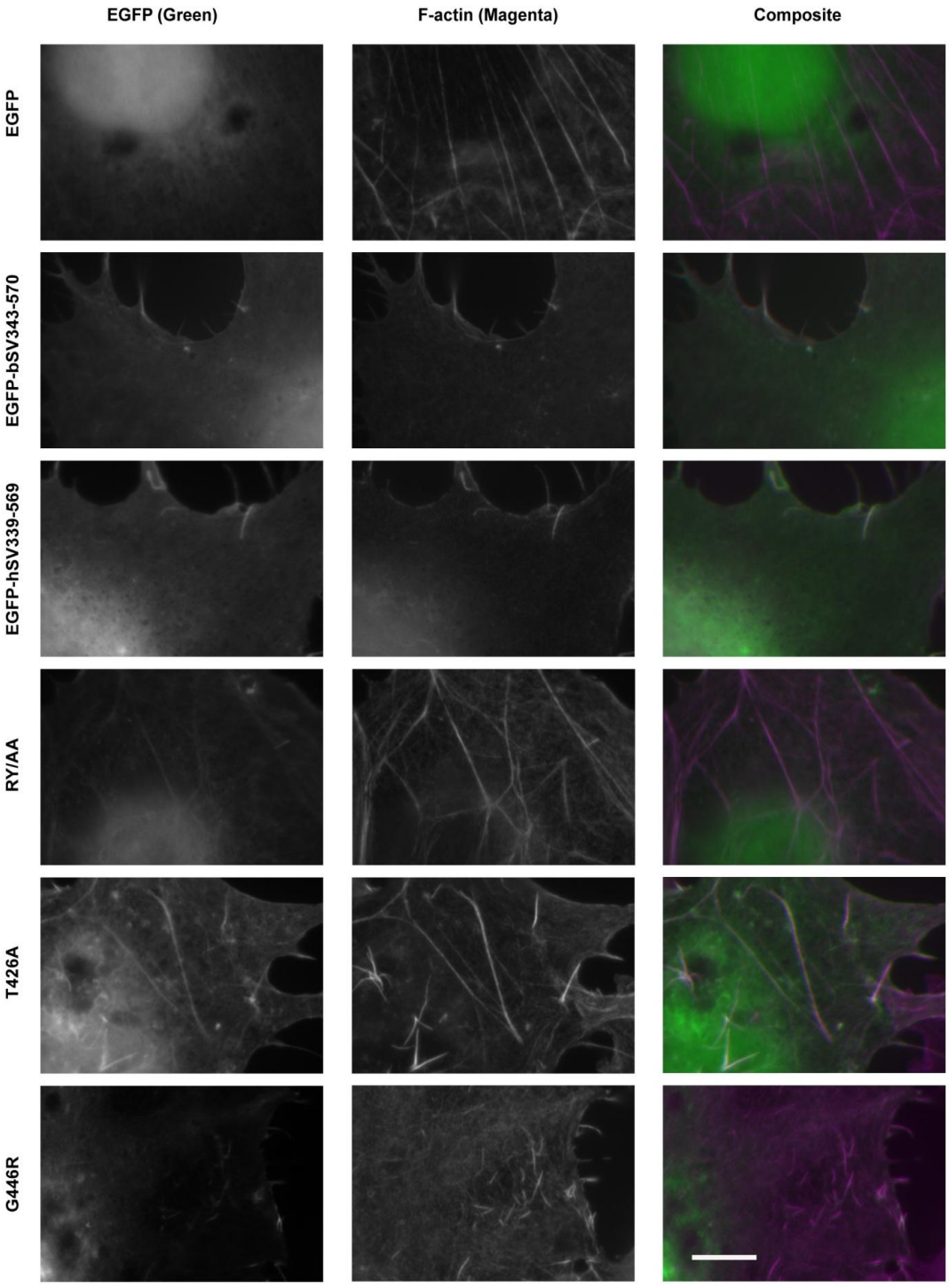


**Figure 7: Representative appearances of transfected cells expressing EGFP only or an EGFP-tagged hSV focal adhesion targeting domain containing the designated mutation.** After 23 hours of transfection using the Effectene protocol (refer to Materials and Methods), cells were fixed with PFA, permeabilized, stained with Texas-red phalloidin, and mounted onto microscope slides. Images were captured at 100X magnification. Bar, 10 µm.

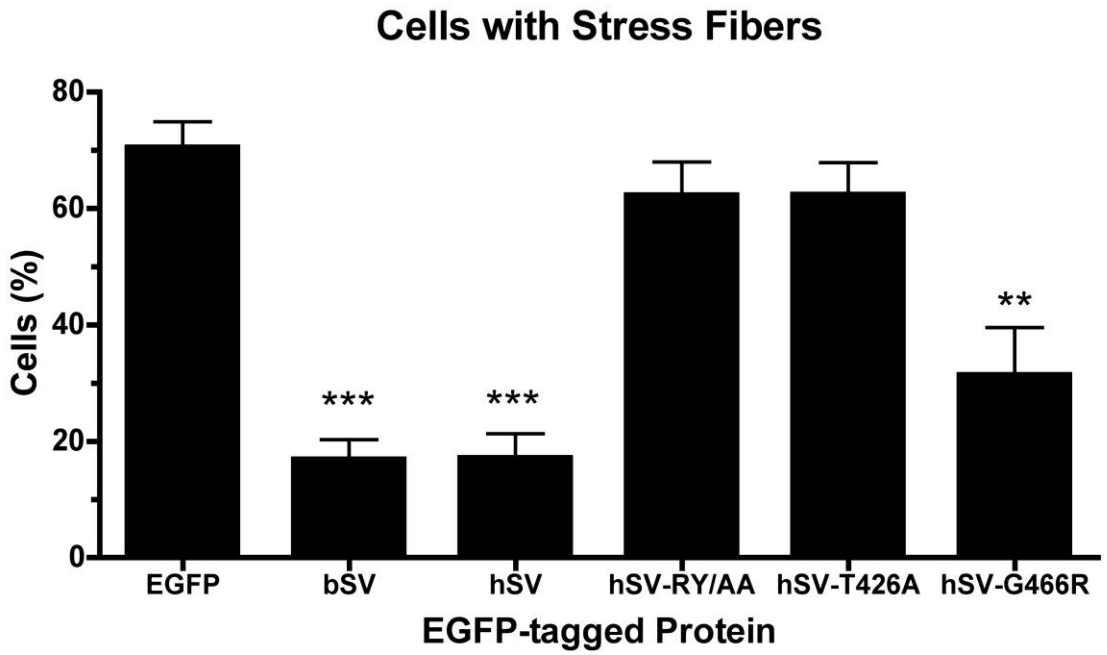


**Figure 8: Histogram of the percentages of COS7-2 cells that contained even one stress fiber.** Means ± S.D. Results that are statistically different from the EGFP control value are designated with asterisks (**P < 0.01, ***P < 0.001).

*Western Immunoblotting*

To confirm that the EGFP-tagged hSV constructs were expressed in the COS 7-2 cells at approximately equal levels, transfected cells were extracted as described in Materials and Methods, and the protein extracts were run on an SDS-polyacrylamide gel, blotted onto a nitrocellulose membrane, and immunostained for EGFP and actin, as a loading control. **Figure 9** shows that all the EGFP-tagged hSV constructs express well and that their expression levels were roughly comparable to that of the EGFP control. **Figure 9A** depicts the EGFP-stained bands for each construct. The band for pEGFP-C1 was at approximately 30 kDa, whereas the hSV proteins are approximately 60 kDa,

which is their predicted molecular mass. The actin bands in Figure 8B are of similar intensity at approximately 40 kDa. Both the EGFP and actin bands in the EGFP control (Fig. 9B, lane 1) are somewhat lighter than the corresponding bands in the EGFP-hSV lanes (Fig. 9B, lanes 2-6), suggesting that the levels of expressed protein are roughly comparable for all 6 proteins. Further analyses of the results are below in the Discussion section.

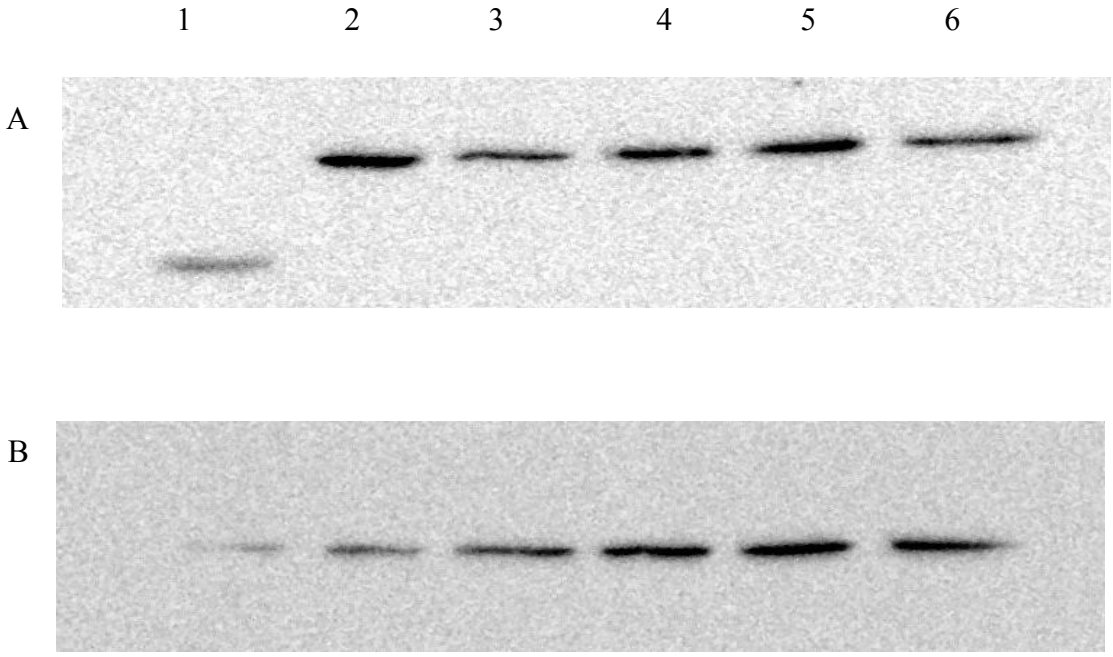


**Figure 9: Protein Expression of (A) EGFP tagged hSV constructs and (B) actin.** For both panels A and B, lanes (1) depicts pEGFP-C1, (2) EGFP-BSV, (3) pEGFP-C1+hSV339-569, (4) pEGFP-C1+hSV339-569-RYAA, (5) pEGFP-C1+ hSV339-569-T426A, and (6) pEGFP-C1+ hSV339-569-G466R.

# DISCUSSION

There are approximately 293 naturally occurring variants present in the human supervillin gene. With several of these in the TRIP6 binding site, the target focal adhesion sequence of human supervillin gene was used to perform multiple PCR reactions including site-directed mutagenesis to create the nucleotide changes depicted in Table 1. As shown in the Results section, the mutant of RY/AA and T426A resulted in similar levels of transfected cells containing stress fibers as that of the EGFP control whereas the G466R, just like the bSV and hSV constructs, mutant decreased the SF count.

As shown in figure 8, my positive and negative controls confirmed previous experiments performed with bSV and bSV fragment proteins. The latter was addressed by transfecting COS7-2 cells with EGFP-tagged hSV and an RY/AA mutant construct. These findings show that the focal adhesion targeting sequence of hSV decreases stress fiber formation to about the same extent as that observed with bSV. In studies completed by Takizawa et al. 2006, the increased levels of cells containing stress fibers for the RY/AA mutant were a result of the inhibition of TRIP6 to regulate bSV binding to focal adhesion (Takizawa et al., 2006). The same thought can be applied to the RY/AA and T426A mutant in hSV due to the fact that human supervillin is expected to down regulate the amount of stress fibers within a cell. Furthermore, the RY/AA mutation eliminates this effect, as it did for bSV (Takizawa et al., 2006). This is expected because of the conserved sequence between the human and bovine species. Successful replication of techniques used throughout this project depicted similar results as previous studies.

Experiments reported here also provided new information about hSV sequences that are important for regulation of focal adhesion function. Through mutating threonine-426 into alanine we observed the reversed inhibition of stress fiber formation as effectively as did the RY/AA mutation (Fig. 8). With a total of 146 observations reported on the PhosphoSitePlus web site, the T426A mutant is the most commonly observed phosphorylated amino acid in the entire human supervillin protein. Results gathered strongly offers poses that phosphorylation at this site is regulatory and with the T426A mutation this phosphorylation mechanism is prevented. Attempts at mutating this site into glutamic acid were performed. Although the latter was unsuccessful due to difficulties with the mutagenesis PCR, preliminary experiments by Dr. Norio Takizawa have shown that the mutation of threonine 426 into glutamic acid in bSV also inhibited the focal adhesion disrupting activity of the FA-targeting fragment. Without the presence of stress fibers, the cells will not be able to adhere to substrates as strongly. The cell will also have a low turnover rate due to the decreased amount of stress fibers.

The second original finding in this project was that the naturally occurring G466R variation within supervillin is likely to affect the function of this protein. The G466R mutation displayed low levels of cells containing stress fibers. This mutant is likely to be less disruptive to focal adhesions than the wild-type hSV fragment. As shown in Figure 8, there is no statistical significance between the values for the G466R mutant and hSV but they are close enough to suggest that additional replicates would result in a functional difference between the two.

Result from the G466R mutant suggests that variations caused by single nucleotide polymorphisms (SNPs) in this region of supervillin may be functionally

significant. The latter would support the GWAS study published by Edelstein et al., where the presence of SNPs in the SVIL gene correlated to differences in platelet adhesion in an African-American population. This study showed that 5 of the top 12 SNPs linked to alterations in platelet function mapped to a region of linkage disequilibrium that includes the target focal adhesion sequence for hSV (investigated in this project; Edelstein et al., 2012). Similar experiments with platelets from a mouse mutant lacking supervillin confirmed that the supervillin-minus platelets were stickier under flow rates identical to those in coronary arteries. Increased adhesion to arterial walls is also linked to increased incidence of heart attack and stroke

Although results received were consistent with expected results and novel findings were received, some problems were encountered during the first triplicate transfections; therefore protein expression levels were analyzed through a western blot. As shown in figure 9, all the EGFP-tagged hSV constructs expressed at approximately equal levels. The later also applies to the anti-actin stain depicting that approximate levels of the protein was loaded onto the gel.

Throughout this project, the target focal adhesion sequence of human supervillin was utilized. Future experiments should include introducing the mutations of RY/AA, T426A, and G466R into full length human supervillin to observe the effect they would have on the cell. Further investigation of this site should be conducted to observe whether other variations in and near the focal adhesion targeting site in supervillin might be predictive of a tendency towards cardiovascular pathology.

# BIBLIOGRAPHY


Bhuwania, R., Cornfine, S., Fang, Z., Krüger, M., Luna, E. J., & Linder, S. (2012). Supervillin couples myosin-dependent contractility to podosomes and enables their turnover. *Journal of cell science*, *125*(Pt 9), 2300–14. doi:10.1242/jcs.100032

Briesewitz, R., Kern, a, & Marcantonio, E. E. (1993). Ligand-dependent and - independent integrin focal contact localization: the role of the alpha chain cytoplasmic domain. *Molecular biology of the cell*, *4*(6), 593–604. Retrieved from http://www.pubmedcentral.nih.gov/articlerender.fcgi?artid=300966&tool=pmcentrez&rendertype=abstract

Burridge, K., & Chrzanowska-wodnicka, M. (1996). Focal Adhesions , Contractility , and Signaling. *Cell and Developmental Biology,12*, 463-519.

Chen, Y., Takizawa, N., Crowley, J. L., Oh, S. W., Gatto, C. L., Kambara, T., Sato, O., et al. (2003). F-actin and myosin II binding domains in supervillin. *The Journal of biological chemistry*, *278*(46), 46094–106. doi:10.1074/jbc.M305311200

Cooper, G. (2000). *The Cell: A Molecular Approach* (2nd ed.). Sunderland: Sinauer Associates.

Cox, L., Umans, L., Cornelis, F., Huylebroeck, D., & Zwijsen, A. (2008). A broken heart: a stretch too far: an overview of mouse models with mutations in stretch-sensor components. *International Journal of Cardiology*, *131*(1), 33–44. doi:10.1016/j.ijcard.2008.06.049

Cutroneo, G., Lentini, S., Favaloro, A., Anastasi, G., & Di Mauro, D. (2011). Costameric proteins: From benchside to future translational cardiovascular research. *Annales de cardiologie et dangeiologie*, *61*(1), 1–6. doi:10.1016/j.ancard.2011.12.003

Ervasti, J. M. (2003). Costameres : the Achilles ' Heel of Herculean Muscle. *The Journal of Biological Chemistry*, *278*(16), 13591–13594. doi:10.1074/jbc.R200021200

Fang, Z., & Luna, E. J. (2013). Supervillin-mediated Suppression of p53 Enhances Cell Survival. *The Journal of biological chemistry*, *288*(11), 7918–7929. doi:10.1074/jbc.M112.416842

Fang, Z., Takizawa, N., Wilson, K. a, Smith, T. C., Delprato, A., Davidson, M. W., Lambright, D. G., et al. (2010). The membrane-associated protein, supervillin, accelerates F-actin-dependent rapid integrin recycling and cell motility. *Traffic (Copenhagen, Denmark)*, *11*(6), 782–99. doi:10.1111/j.1600-0854.2010.01062.x

Fanin, M., Duggan, D. J., Mostacciuolo, M. L., Martinello, F., Freda, M. P., Sorarù, G., Trevisan, C. P., et al. (1997). Genetic epidemiology of muscular dystrophies

resulting from sarcoglycan gene mutations. *Journal of medical genetics*, *34*(12), 973–7. Retrieved from: http://www.pubmedcentral.nih.gov/articlerender.fcgi?artid=1051145&tool=pmcentrez&rendertype=abstract

Fedechkin, S.O., Brockerman, J., Luna , E. J., Lobanov, M. Y., Galzitskaya, O. V. & Smirnov, S.L. (2012): An N-terminal, 830 residues intrinsically disordered region of the cytoskeletonregulatory protein supervillin contains Myosin II- and F-actin-binding sites, Journal of Biomolecular Structure and Dynamics,doi: 10.1080/07391102.2012.726531

Galbraith, C. G., Yamada, K. M., & Galbraith, J. A. (2013). Polymerizing Actin Fibers Integrins Primed to Probe Adhesion Position for Adhesion sites. *Science*, *315*(5814), 992–995.

Geiger, B., Salomon, D., Takeichi, M., & Hynes, R. O. (1992). A chimeric N-cadherin/beta 1-integrin receptor which localizes to both cell-cell and cell-matrix adhesions. *Journal of cell science*, *103 ( Pt 4)*, 943–51. Retrieved from http://www.ncbi.nlm.nih.gov/pubmed/1283166

Godaly, G., Bergsten, G., Hang, L., Fischer, H., Frendéus, B., Lundstedt, a C., Samuelsson, M., et al. (2001). Neutrophil recruitment, chemokine receptors, and resistance to mucosal infection. *Journal of leukocyte biology*, *69*(6), 899–906. Retrieved from http://www.ncbi.nlm.nih.gov/pubmed/11404374

Höner, B., Citi, S., Kendrick-Jones, J., & Jockusch, B. M. (1988). Modulation of cellular morphology and locomotory activity by antibodies against myosin. *The Journal of cell biology*, *107*(6 Pt 1), 2181–9. Retrieved from http://www.pubmedcentral.nih.gov/articlerender.fcgi?artid=2115695&tool=pmcentrez&rendertype=abstract

Huxley, H., & Hanson, J. (1954). Changes in the Cross-Striations of Muscle during Contraction and Stretch and their SAtructural Interpretation. *Nature, 173*, 973-976.

Kanchanawong, P., Shtengel, G., Pasapera, A. M., Ramko, E. B., Davidson, M. W., Hess, H. F., & Waterman, C. M. (2010). Nanoscale architecture of integrin-based cell adhesions. *Nature*. Nature Publishing Group. Retrieved from http://www.pubmedcentral.nih.gov/articlerender.fcgi?artid=3046339&tool=pmcentrez&rendertype=abstract

King, M. (2013). *Muscle Fibers*. Retrieved from The Medical Biochemistry Page: http://themedicalbiochemistrypage.org/muscle.php

LaFlamme, S. E., Akiyama, S. K., & Yamada, K. M. (1992). Regulation of fibronectin receptor distribution. *The Journal of cell biology*, *117*(2), 437–47. Retrieved from

http://www.pubmedcentral.nih.gov/articlerender.fcgi?artid=2289425&tool=pmcentrez&rendertype=abstract

Lo, S. H. (2006). Focal adhesions: what's new inside. *Developmental biology*, *294*(2), 280–91. doi:10.1016/j.ydbio.2006.03.029

Luxenburg, C., Winograd-Katz, S., Addadi, L., & Geiger, B. (2012). Involvement of actin polymerization in podosome dynamics. *Journal of cell science*, *125*(Pt 7), 1666–72. doi:10.1242/jcs.075903

Oh, S. W., Pope, R. K., Smith, K. P., Crowley, J. L., Nebl, T., Lawrence, J. B., & Luna, E. J. (2003). Archvillin, a muscle-specific isoform of supervillin, is an early expressed component of the costameric membrane skeleton. *Journal of cell science*, *116*(Pt 11), 2261–75. doi:10.1242/jcs.00422

Pestonjamasp, K. N., Pope, R. K., Wulfkuhle, J. D., & Luna, E. J. (1997). Supervillin (p205): A novel membrane-associated, F-actin-binding protein in the villin/gelsolin superfamily. *The Journal of cell biology*, *139*(5), 1255–69. Retrieved from http://www.pubmedcentral.nih.gov/articlerender.fcgi?artid=2140202&tool=pmcentrez&rendertype=abstract

Pope, R. K., Pestonjamasp, K. N., Smith, K. P., Wulfkuhle, J. D., Strassel, C. P., Lawrence, J. B., & Luna, E. J. (1998). Cloning, Characterization, and Chromosomal Localization of Human Supervillin ( SVIL ). *Genomics*, *351*, 342–351.

Samarel, A. M. (2005). Costameres, focal adhesions, and cardiomyocyte mechanotransduction. *American journal of physiology. Heart and circulatory physiology*, *289*(6), H2291–301. doi:10.1152/ajpheart.00749.2005

Schürpf, T., & Springer, T. a. (2011). Regulation of integrin affinity on cell surfaces. *The EMBO journal*, *30*(23), 4712–27. doi:10.1038/emboj.2011.333

Smith, T. C., Fang, Z., & Luna, E. J. (2010). Novel interactors and a role for supervillin in early cytokinesis. *Cytoskeleton (Hoboken, N.J.)*, *67*(6), 346–64. doi:10.1002/cm.20449

Takizawa, N., Ikebe, R., Ikebe, M., & Luna, E. J. (2007). Supervillin slows cell spreading by facilitating myosin II activation at the cell periphery. *Journal of Cell Science*, *120*(Pt 21), 3792–3803. doi:10.1242/jcs.008219

Takizawa, N., Smith, T. C., Nebl, T., Crowley, J. L., Palmieri, S. J., Lifshitz, L. M., Ehrhardt, A. G., Hoffman, L. M., Beckerle, M. C., Luna, E. J. (2006). Supervillin modulation of focal adhesions involving TRIP6/ZRP-1. *The Journal of Cell Biology*, *174*(3), 447–458. doi:10.1083/jcb.200512051

Towbin, H., Staehelin, T., & Gordon, J. (1979). Electrophoretic transfer of proteins from polyacrylamide gels to nitrocellulose sheets: procedure and some applications. 1979. *Proceedings of the National Academy of Sciences*, *76*(9), 4350–4354. Retrieved from http://www.ncbi.nlm.nih.gov/pubmed/1422008

Wehrle-Haller, B. (2012a). Assembly and disassembly of cell matrix adhesions. *Current Opinion in Cell Biology*, *null*(Figure 1), 1–10. Retrieved from http://www.ncbi.nlm.nih.gov/pubmed/22819513

Wehrle-Haller, B. (2012b). Structure and function of focal adhesions. *Current opinion in cell biology*, *24*(1), 116–24. doi:10.1016/j.ceb.2011.11.001

Wulfkuhle, J. D., Donina, I. E., Stark, N. H., Pope, R. K., Pestonjamasp, K. N., Niswonger, M. L., & Luna, E. J. (1999). Domain analysis of supervillin, an F-actin bundling plasma membrane protein with functional nuclear localization signals. *Journal of cell science*, *112 ( Pt 13)*, 2125–36. Retrieved from http://www.ncbi.nlm.nih.gov/pubmed/10362542

Yamada, K. M., & Miyamoto, S. (1995). Integrin transmembrane signaling and cytoskeletal control. *Current opinion in cell biology*, *7*(5), 681–9. Retrieved from http://www.ncbi.nlm.nih.gov/pubmed/8573343

Ylainne, J., Chen, Y., Toole, T. E. O., Loftus, J. C., Takada, Y., & Ginsberg, M. H. (1993). Distinct Functions of Integrin alpha and beta Subunit Cytoplasmic Domains in Cell Spreading and Formation of Focal Adhesions. *The Journal of Cell Biology*, *122*(1), 223–233.